Epithelial EZH2 serves as an epigenetic determinant in experimental colitis by inhibiting TNFα-mediated inflammation and apoptosis

Yongfeng Liu[a,b,1], Junjie Peng[c,1], Tongyu Sun[a,1], Ni Li[a], Le Zhang[d], Jiale Ren[a], Huairui Yuan[a], Shan Kan[a], Qiang Pan[a], Xiang Li[a], Yufeng Ding[a], Min Jiang[a], Xiaoji Cong[e], Minjia Tan[e], Yushui Ma[f], Da Fu[f], Sanjun Cai[c], Yichuan Xiao[g], Xiaoming Wang[d], and Jun Qin[a,b,2]

[a]The Key Laboratory of Stem Cell Biology, CAS Center for Excellence in Molecular Cell Science, Institute of Health Sciences, Shanghai Institutes for Biological Sciences, Chinese Academy of Sciences and Shanghai Jiao Tong University School of Medicine, University of Chinese Academy of Sciences, Shanghai 200031, China; [b]State Key Laboratory of Pharmaceutical Biotechnology, Nanjing University, Nanjing 210023, China; [c]Department of Colorectal Surgery, Fudan University Shanghai Cancer Center, Shanghai 200032, China; [d]Department of Immunology, Nanjing Medical University, Nanjing 211166, China; [e]State Key Laboratory of Drug Research, Shanghai Institute of Materia Medica, Chinese Academy of Sciences, Shanghai 201203, China; [f]Central Laboratory for Medical Research, Shanghai Tenth People's Hospital, Tongji University School of Medicine, Shanghai 200072, China; and [g]The Key Laboratory of Stem Cell Biology, Institute of Health Sciences, Shanghai Institutes for Biological Sciences, Chinese Academy of Sciences and Shanghai Jiao Tong University School of Medicine, Shanghai 200031, China

Edited by Richard A. Flavell, Yale School of Medicine Howard Hughes Medical Institute, New Haven, CT, and approved April 4, 2017 (received for review January 18, 2017)

Epithelial barrier disruption is a major cause of inflammatory bowel disease (IBD); however, the mechanism through which epigenetic regulation modulates intestinal epithelial integrity remains largely undefined. Here we show that EZH2, the catalytic subunit of polycomb repressive complex (PRC2), is indispensable for maintaining epithelial cell barrier integrity and homeostasis under inflammatory conditions. In accordance with reduced EZH2 expression in patients, the inactivation of EZH2 in IECs sensitizes mice to DSS- and TNBS-induced experimental colitis. Conversely, EZH2 overexpression in the intestinal epithelium renders mice more resistant to colitis. Mechanistically, the genes encoding TRAF2/5 are held in a finely tuned bivalent status under inflammatory conditions. EZH2 deficiency potentiates the expression of these genes to enhance TNFα-induced NF-κB signaling, thereby leading to uncontrolled inflammation. More importantly, we show that EZH2 depletion compromises the protective role of NF-κB signaling in cell survival by directly up-regulating ITCH, a well-known E3 ligase that degrades the c-FLIP protein. Thus, our findings highlight an epigenetic mechanism by which EZH2 integrates the multifaceted effects of TNFα signaling to promote the inflammatory response and apoptosis in colitis.

colitis | EZH2 | TNFα | NF-κB | ITCH

Intestinal immune homeostasis depends on tightly regulated crosstalk among commensal bacteria, mucosal immune cells, and intestinal epithelial cells (IECs). Disruption of this homeostasis leads to inflammatory bowel disease (IBD), an inflammatory disorder of the gastrointestinal tract, which is typically classified as Crohn's disease (CD) or ulcerative colitis (UC) (1).

An unrestrained inflammatory response and aberrant apoptosis of IECs are major contributing factors in the pathogenesis of IBD. By separating luminal bacteria from underlying immune cells, IECs form the mucosal barrier and play critical roles in gut immune homeostasis (2, 3). Excess IEC apoptosis is frequently observed in patients with IBD and leads to a disruption of intestinal barrier integrity (3, 4), thereby allowing the translocation of luminal antigens and bacteria into the lamina propria and triggering a chronic inflammatory response. This response is characterized by the recruitment of immune cells and the production of proinflammatory cytokines via the activation of transcription factors, such as NF-κB (5, 6). These cytokines typically clear invading bacteria and protect the body from infection; however, under pathogenic conditions, they induce IEC death and further impair epithelial integrity, thereby creating a vicious cycle and eventually leading to IBD (3, 7–9). Among the cytokines implicated in colitis, TNFα is the best studied, and its overproduction is a hallmark of IBD. Thus, anti-TNFα therapies have been adopted to reduce inflammatory responses and apoptosis in the treatment of IBD (10). As a pleiotropic cytokine, TNFα not only induces IEC apoptosis by inducing the cleavage of caspase 8 or PUMA (11), but also stimulates NF-κB signaling to augment the immune response. Intriguingly, activated NF-κB induces a subset of prosurvival genes, including c-FLIP, a critical inhibitor of caspase 8, to antagonize apoptosis (12). Therefore, TNFα has proapoptotic and antiapoptotic effects. How this complex behavior promotes disease progression during IBD pathogenesis remains to be elucidated.

Alterations to chromatin are central to the reprogramming of pathological gene expression, which is directly relevant to many inflammatory diseases, including IBD (2, 13, 14). Studies have shown that DNA methylation is well correlated with various aspects of IBD, including disease duration and severity of inflammation (15, 16). It is also known that the expression of histone deacetylase 3 (HDAC3), an epigenome-modifying enzyme, influences

Significance

TNFα is the key cytokine implicated in inflammatory bowel disease. However, TNFα is not always proinflammatory, because TNFα-activated NF-κB induces prosurvival proteins, including c-FLIP, to constrain caspase 8 activation. Here we report that epithelial EZH2 integrates the multifaceted effects of TNFα signaling to promote inflammation and apoptosis in colitis. EZH2 reduction directly stimulates TRAF2/5 expression to enhance TNFα-induced NF-κB signaling. More importantly, EZH2 deficiency up-regulates the expression of the E3 ligase ITCH to degrade the c-FLIP protein, thereby antagonizing the prosurvival role of NF-κB. Taken together, our results indicate that EZH2 serves as an epigenetic brake to modulate TNFα functions in colitis. Moreover, the data suggest that patients with lower levels of EZH2 might have a better response to anti-TNFα therapy.

Author contributions: J.Q. designed research; Y.L., J.P., T.S., N.L., L.Z., J.R., H.Y., S.K., Q.P., X.L., Y.D., X.C., Y.M., and D.F. performed research; Y.L., J.P., N.L., M.J., M.T., D.F., S.C., Y.X., X.W., and J.Q. analyzed data; and Y.L., X.W., and J.Q. wrote the paper.

The authors declare no conflict of interest.

This article is a PNAS Direct Submission.

Data deposition: The data reported in this paper have been deposited in the Gene Expression Omnibus (GEO) database, https://www.ncbi.nlm.nih.gov/geo (accession nos. GSE84857 and GSE84858).

[1]Y.L., J.P., and T.S. contributed equally to this work.

[2]To whom correspondence should be addressed. Email: qinjun@sibs.ac.cn.

This article contains supporting information online at www.pnas.org/lookup/suppl/doi:10.1073/pnas.1700909114/-/DCSupplemental.

the susceptibility to multiple systemic chronic inflammatory diseases (2). Of note, interest in histone methyltransferases (HMTases) is growing owing to their enzymatic activity and therapeutic potential (17–19). As one of the major histone modifications, extensive alteration of H3K27me3 (histone H3 trimethylation of Lys-27) has been reported following an inflammatory insult, with a specific reduction during the progression of experimental colitis (20). H3K27me3 marks are associated with gene silencing and are added to histones predominantly via polycomb repressive complex 2 (PRC2). This complex comprises the methyltransferases EZH1 or EZH2, as well as the structural proteins EED, SUZ12, and RBBP7/4 (21). Recent studies have revealed that PRC2 activity is required for intestinal epithelial homeostasis (22–24). EED deficiency has been observed to impair stem cell proliferation and lead to abnormal secretory lineage commitment. Such epithelial defects were detected in EED-depleted mice, but not in EZH2 KO mice, an effect likely due to the functional redundancy between EZH2 and EZH1 (24). However, EZH2 has higher enzymatic activity than EZH1 and is more frequently dysregulated in tumors compared with other components of PRC2, suggesting some unique functional properties (24). Interestingly, a study applying a rank-based expression profile comparative algorithm between UC patients and siRNA-treated cells identified EZH2 as one of the top candidates for involvement in IBD (25). Nevertheless, experimental evidence is lacking to directly address the role of EZH2 in the pathogenesis of IBD.

In the present work, we have established that epithelial EZH2 is important for the pathogenesis of colitis. Mechanistically, our results highlight EZH2 as a critical epigenetic determinant in the prevention of colitis through modulation of TNFα-dependent inflammatory response and apoptosis.

Results

EZH2 Expression Is Decreased in IBD Patients. Given the potential importance of colonic EZH2 in the pathogenesis of IBD, we analyzed EZH2 mRNA expression in public gene datasets of CD and UC samples. The results indicate that EZH2 was downregulated in these samples compared with samples from healthy controls, whereas no significant differences were observed for other components of PRC2, such as EZH1 and EED (Fig. 1*A*). To expand on these observations, we examined EZH2 expression in colonic biopsy specimens from CD and UC patients as well as from normal controls. Consistent with the results obtained from dataset mining, qRT-PCR analysis indicated significantly reduced EZH2 expression in IBD patients compared with healthy subjects (Fig. 1*B*).

To further assess the clinical relevance of EZH2 in IBD, we performed immunohistochemistry analyses to characterize EZH2 expression at the cellular level. Immunostaining revealed high expression of EZH2 in normal colonic epithelial cells, but significantly lower expression in the epithelium of both CD and UC biopsy specimens (Fig. 1*C*). Taken together, these results suggest that EZH2 reduction in colorectal epithelium is associated with the pathogenesis of IBD.

EZH2$^{IEC-/-}$ Mice Are Highly Susceptible to DSS-Induced Colitis. To assess the role of epithelial EZH2 in colitis, EZH2-flox mice were crossed with Villin-Cre mice to generate IEC-specific EZH2-deficient mice (Villin-Cre; EZH2 Flox/Flox mice, hereinafter referred to as EZH2$^{IEC-/-}$ mice). As expected, EZH2 was efficiently ablated and H3K27me3 was substantially reduced in the intestinal epithelium of EZH2$^{IEC-/-}$ mice (Fig. 2*A*). Consistent with previous reports (24), EZH2$^{IEC-/-}$ mice displayed normal intestinal histology, and both stem/progenitor cell proliferation and terminally differentiated cells were indistinguishable between wild-type and EZH2$^{IEC-/-}$ mice under steady-state conditions (Fig. S1*A*). In addition, assessment of the numbers of goblet cells, enterocytes, and Paneth cells [identified by periodic acid–Schiff (PAS), alkaline phosphatase (ALP), and lysozyme staining, respectively] revealed no obvious differences in terms of cell lineage commitment (Fig. S1*B*). This observation was further confirmed by qRT-PCR analysis, which showed no significant alterations in the expression of marker genes for the different cell lineages and stem cell populations in EZH2-deficient intestinal tissue compared with control tissue (Fig. S1*C*).

Dextran sulfate sodium (DSS)-induced colitis is a commonly used mouse model that mimics the clinical pathology of IBD (26). We challenged wild-type and EZH2-deficient mice with 3% DSS and then monitored their susceptibility by measuring body weight and colon length and assessing rectal bleeding. We found that EZH2$^{IEC-/-}$ mice lost significantly more body weight in response to DSS treatment compared with the control cohort, and macroscopic dissection revealed significantly shorter colons in the EZH2$^{IEC-/-}$ mice compared with the wild-type mice (Fig. 2 *B* and *C*). On further histopathological examination, the EZH2$^{IEC-/-}$ mice exhibited widespread damage in the distal-middle portion of the colon, with extensive epithelial denudation and more ulcerations compared with wild-type mice, which showed partially preserved epithelial structures (Fig. 2*D*). In

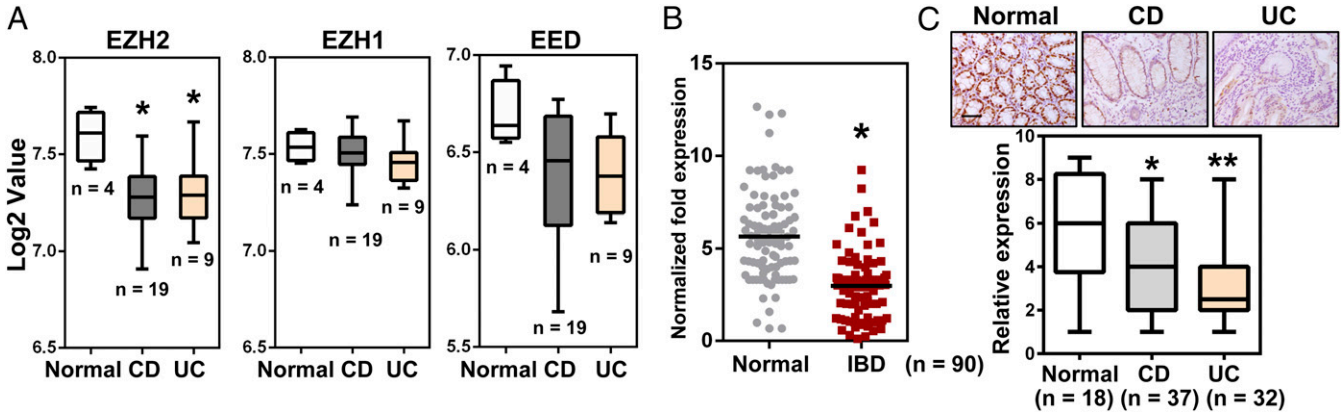

Fig. 1. The clinical relevance of EZH2 in IBD patients. (*A*) Boxplot of EZH2, EZH1, and EED expression levels in healthy controls, CD patients, and UC patients (using dataset GSE6731; $n = 32$). (*B*) qRT-PCR analysis of EZH2 transcripts in IBD specimens and healthy subjects ($n = 90$). (*C*) Immunohistochemical examination of EZH2 protein in UC, CD, and healthy samples, as indicated. (*Upper*) Representative EZH2 staining results. (*Lower*) Boxplot of EZH2 staining indices using a 10-point quantification scale. The Wilcoxon signed-rank test was used to calculate the expression index. (Scale bars: 50 μm.)

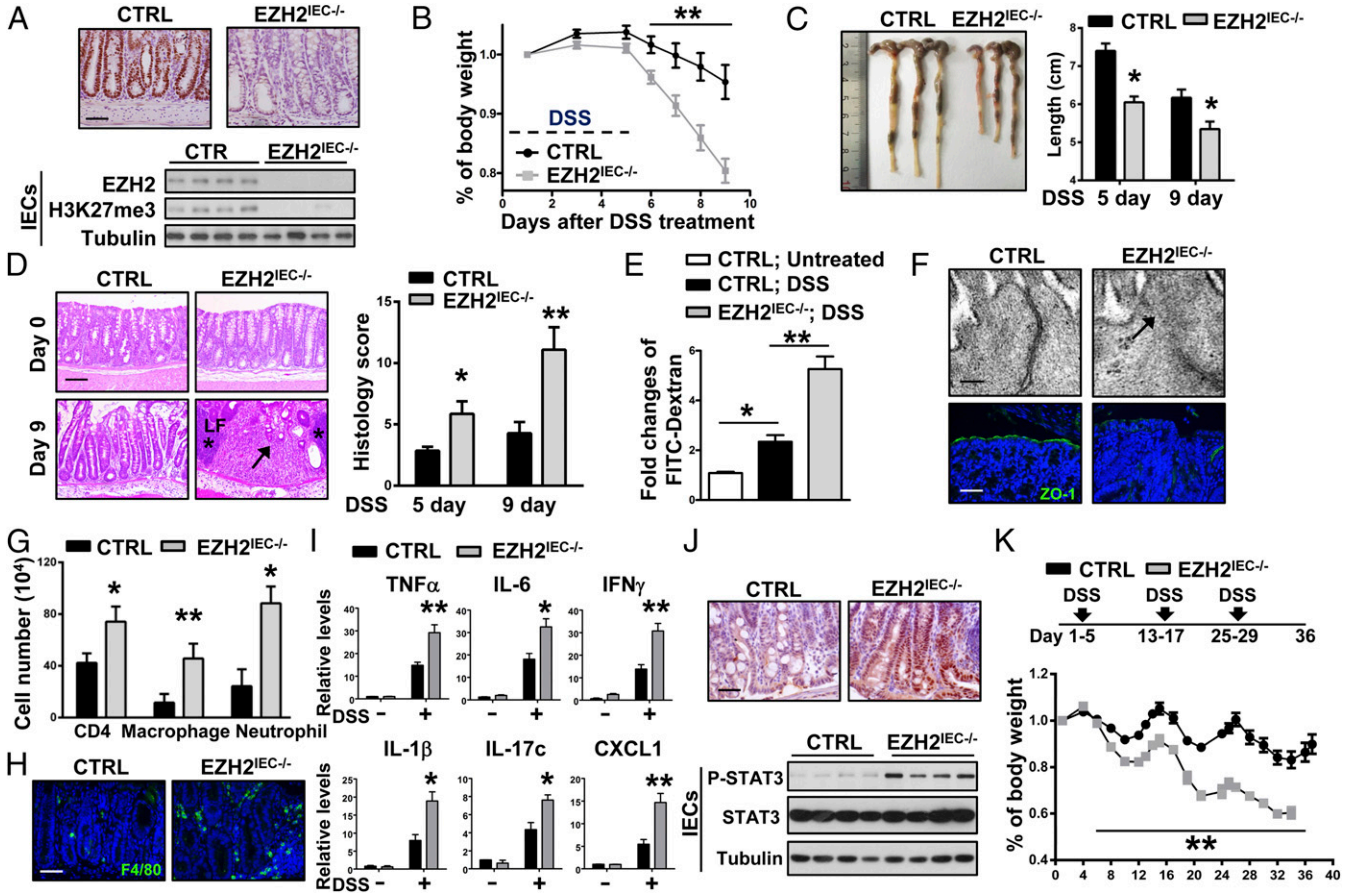

Fig. 2. Loss of EZH2 in IECs aggravates DSS-induced colitis in mice. (*A*) Immunohistochemical (*Upper*) and immunoblot (*Lower*) analyses of EZH2 expression. (*B*) Wild-type control (CTRL) and EZH2$^{IEC-/-}$ mice were fed 3% DSS in drinking water for 5 d, and body weights were scored daily (n >9 per group). (*C*) The mice were euthanized on days 5 and 9 to measure colon length. (*D*, *Left*) H&E- stained sections of middle-distal colon tissue collected at days 0 and 9. (*D*, *Right*) Semiquantitative scoring of the histopathology. Asterisks denote isolated lymphoid follicles; arrows, infiltration of immune cell and epithelial cell damage (n > 5 per group). (*E*) Intestinal permeability measured by the concentration of FITC-dextran in the blood serum (n > 5). (*F*) Representative electron microscope images (*Upper*) and ZO-1 staining (*Lower*) in colon sections of mice treated with DSS for 5 d. (*G*) After 5 d of DSS treatment, colonic lamina propria cells were analyzed by flow cytometry for CD4$^+$ T cells, CD11b$^+$; F4/80$^+$ macrophages, and CD11b$^+$; Gr-1$^+$ neutrophils (n = 3). (*H*) F4/80 staining in a noninflamed portion of the colon at day 5 of DSS treatment. (*I*) qRT-PCR analysis of whole colon homogenates to assess cytokine and chemokine production (5 d of DSS treatment; n = 5). (*J*) STAT3 phosphorylation on Tyr705 in representative colon sections (*Upper*) and Western blot analysis of colon tissues (*Lower*), as indicated. (*K*) Body weight changes in the mice during three cycles of 3% DSS treatment. *P < 0.05; **P < 0.01. (Scale bars: 50 μm in *A*, *F*, *Lower*, *H*, and *J*; 100 μm in *D*; 100 nm in *F*, *Upper*.)

accordance with the severe ulceration observed in EZH2-depleted mice, intestinal permeability was markedly increased in these animals, based on a serum FITC-dextran analysis (Fig. 2*E*).

Because tight junctions are pivotal in regulating intestinal permeability, we performed electron microscopy analysis to examine whether the loss of EZH2 alters tight junctions. In contrast to the findings in wild-type mice, tight junctions were morphologically disrupted or discontinuous and had lower electron densities on the apical surfaces of EZH2-depleted epithelia (Fig. 2*F*, *Upper*, arrow). We also examined the distribution of the tight junction protein 1 (ZO-1) in control and EZH2$^{IEC-/-}$ mice as a marker of tight junction structure. Immunostaining of control colons revealed partially disrupted but relatively normal ZO-1 distributions; however, focal regions of diminished or discontinuous ZO-1 staining were observed in EZH2-depleted colons (Fig. 2*F*, *Lower*). These results indicate that an intact and functional mucosal barrier was compromised in EZH2$^{IEC-/-}$ mice.

We then analyzed immune cell infiltration by flow cytometry. During the early stages of colitis (at day 5), we observed increased numbers of CD4$^+$ T cells, neutrophils, and macrophages in EZH2$^{IEC-/-}$ mice compared with control mice (Fig. 2*G*). Notably, the hyperinfiltration of immune cells in the EZH2$^{IEC-/-}$ mice was not confined to inflamed areas but extended to the entire colon, as evidenced by increased F4/80-positivity in relatively noninflamed portions of the EZH2$^{IEC-/-}$ colons (Fig. 2*H*). The expression levels of proinflammatory cytokines and chemokines were consistently prominently elevated in DSS-treated EZH2$^{IEC-/-}$ mice, whereas basal levels of these cytokines in untreated mice were comparable (Fig. 2*I*). The excessive immune response seen in EZH2-deficient mice was further confirmed by immunostaining of colon sections for phospho-STAT3 and immunoblotting of isolated IECs from control and EZH2$^{IEC-/-}$ mice (Fig. 2*J*). Finally, we assessed the role of EZH2 in chronic colitis by subjecting the mice to three cycles of DSS treatment, with each cycle consisting of 5 d of DSS water followed by 7 d of water alone. EZH2 depletion also aggravated disease severity in this chronic colitis model (Fig. 2*K*). Collectively, our results demonstrate that epithelial EZH2 functions as a defense mechanism to prevent DSS-induced colitis.

EZH2 Deficiency Sensitizes Mice to TNBS-Induced Colitis. Having identified the essential role of EZH2 in DSS-induced colitis, we used another disease model to substantiate this idea. The

2,4,6-trinitrobenzene sulfonic acid (TNBS)-induced colitis model acts via acute destruction of the intestinal barrier and involves Th1-mediated mucosal inflammation, thereby mimicking CD in humans (27, 28). We challenged wild-type and EZH2$^{IEC-/-}$ mice with TNBS to assess the role of epithelial EZH2 in this model. We found that EZH2$^{IEC-/-}$ mice were more susceptible than wild-type mice to TNBS-induced colitis. As shown in Fig. 3*A*, the intrarectal administration of TNBS resulted in gradual weight loss in control mice over the first 3 d, followed by recovery thereafter. In contrast, EZH2-deficient mice experienced significantly greater weight loss. By day 5, EZH2$^{IEC-/-}$ mice exhibited symptoms of severe colitis disease activity, including severe diarrhea, rectal bleeding, and marked colon shortening (Fig. 3*B*).

This clinical manifestation of increased colorectal inflammation in EZH2$^{IEC-/-}$ mice was further supported by the results of histopathological analyses. Specifically, H&E-stained colon sections of EZH2$^{IEC-/-}$ mice revealed extensive inflammation in the lamina propria as well as severe colonic damage (Fig. 3*C*, *Upper*). Similarly, there were significantly more infiltrated macrophages in noninflamed areas of EZH2-deficient colon sections (Fig. 3*C*, *Lower*). Moreover, increased local production of several inflammatory cytokines was detected in the KO mice (Fig. 3*D*). Accordingly, phospho-STAT3 levels were elevated in colon homogenates of EZH2$^{IEC-/-}$ mice compared with wild-type mice (Fig. 3*E*). Taken together, these results indicate that depletion of EZH2 leads to exacerbated colitis.

Overexpression of EZH2 in IECs Protects Mice from DSS-Induced Colitis. We next aimed to determine whether elevated EZH2 expression in IECs can protect mice from colitis. Accordingly, we generated conditional EZH2 overexpressing mice (EZH2$^{OE/+}$), which carry a single copy of a mini-gene consisting of a CAGGS (hybrid chicken β-actin and cytomegalovirus) promoter, a loxP-STOP-loxP cassette, and myc-tagged EZH2 cDNA knocked into the Rosa26 locus (Fig. 4*A*, *Upper* and Fig. S2*A*). As expected, EZH2$^{OE/+}$ mice were generally healthy in terms of growth and reproduction. On crossing these mice with Villin-Cre mice, EZH2 was exclusively overexpressed in IECs (hereafter referred as EZH2$^{IECOE/+}$). Western blot analyses revealed a threefold to fourfold increase in EZH2 expression in colon homogenates of EZH2$^{IECOE/+}$ mice compared with control mice (Fig. 4*A*, *Lower*). Further immunostaining with anti-Myc and EZH2 antibodies verified that EZH2 was induced predominantly in IECs (Fig. S2*B*).

Next, we treated control and EZH2$^{IECOE/+}$ mice with DSS as described above. Mice overexpressing EZH2 in IECs developed significantly less colonic inflammation. By day 9, wild-type mice showed colitis activity, as evidenced by diarrhea, severe body weight loss, and marked shortening and thickening of the colon. In sharp contrast, EZH2$^{IECOE/+}$ mice developed almost no symptoms, and their large bowel showed few signs of colitis (Fig. 4 *B* and *C*). Histological examination revealed obvious crypt loss, focal ulceration, and inflammation in the wild-type colons, compared with very little damage and less histological inflammation in the EZH2$^{IECOE/+}$ colons (Fig. 4*D*). Similarly, the colon homogenates of EZH2$^{IECOE/+}$ mice contained significantly lower proinflammatory cytokine levels compared with control mice (Fig. 4*E*). Taken together, our gain-of-function results complement those obtained from the EZH2-KO mice, strongly suggesting that epithelial EZH2 expression is highly protective against experimental colitis in vivo.

EZH2 Inhibits TNFα-Mediated NF-κB Activation in Experimental Colitis. To understand the mechanistic role of EZH2 in colitis, we conducted a gene expression profile analysis using primary colorectal IECs isolated from wild-type and EZH2$^{IEC-/-}$ mice at 3 d after DSS treatment. At that time point, EZH2$^{IEC-/-}$ mice did not exhibit morphological defects; therefore, the genes exhibiting altered expression levels might be closely and more directly related to earlier events regulated by EZH2. Gene Ontology analysis revealed that the most prominently altered biological processes were associated with immunologic and inflammatory

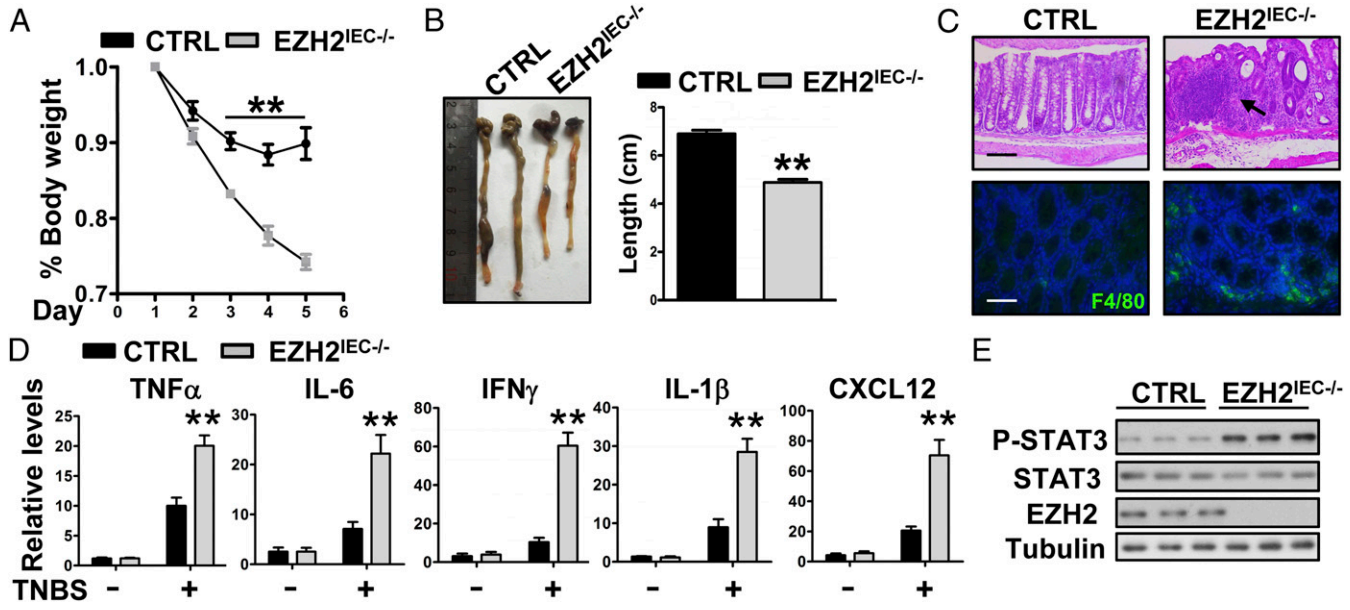

Fig. 3. EZH2-deficient mice are more susceptible to TNBS-induced colitis. (*A*) Body weight changes in control and EZH2$^{IEC-/-}$ mice after TNBS treatment ($n = 5$ per group). (*B*) Colon lengths in the mice after 5 d of TNBS treatment. (*C*) Representative H&E-stained colon sections (*Upper*) and F4/80 staining of noninflamed sections (*Lower*) of control (CTRL) and EZH2$^{IEC-/-}$ mice after 5 d of TNBS treatment. The arrow indicates the infiltration of immune cell and epithelial cell damage. (Scale bars: 200 μm in *Upper*; 50 μm in *Lower*). (*D*) Relative mRNA levels for the indicated genes in the distal colons of untreated and TNBS-treated control and EZH2$^{IEC-/-}$ mice (day 5; $n = 5$). (*E*) Immunoblot analysis of the indicated protein in the distal colons of TNBS-treated mice. *$P < 0.05$; **$P < 0.01$.

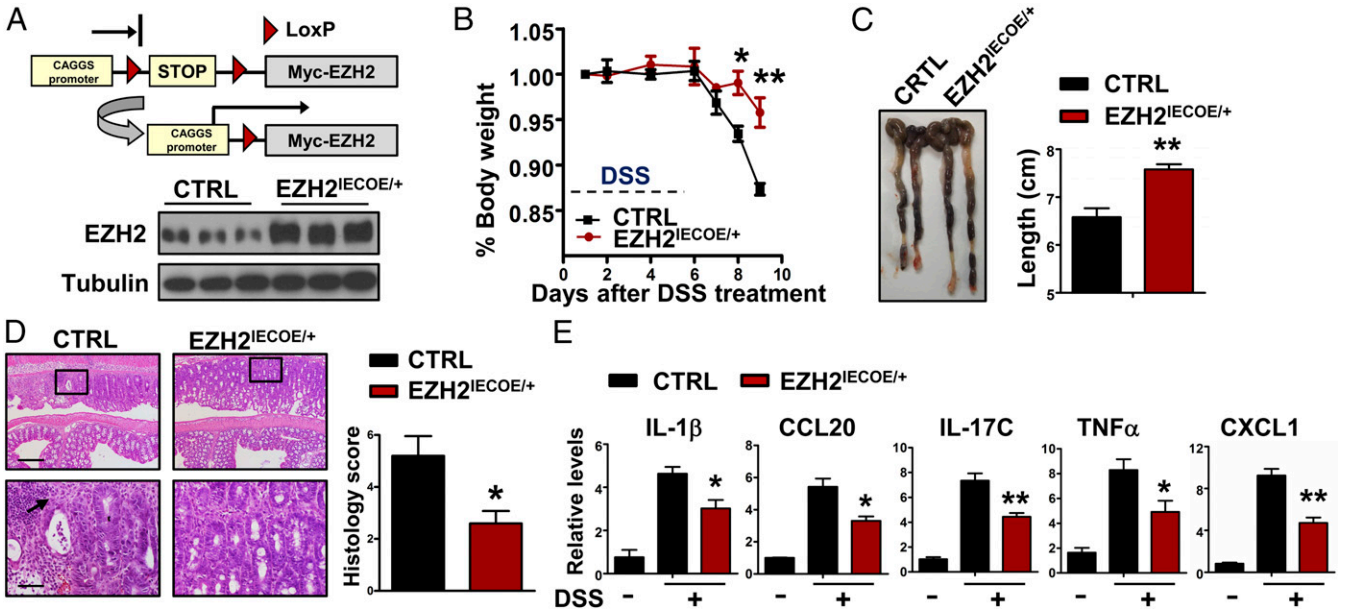

Fig. 4. Overexpression of EZH2 in IECs protects mice from DSS-induced colitis. (*A*) Scheme of conditional overexpression of EZH2 mice (*Upper*) and Western blot analysis of EZH2 expression in colonic homogenates of control (CTRL) and EZH2$^{IECOE/+}$ mice (*Lower*). (*B* and *C*) After the addition of DSS to the drinking water for 5 d, body weights (*B*) and colon lengths (*C*) were recorded ($n = 5$). (*D*, *Left*) Representative H&E-stained middle-distal colon sections of control and EZH2$^{IECOE/+}$ mice treated with DSS for 5 d. The arrow indicates the infiltration of immune cells. (*D*, *Right*) Semiquantitative scoring of the histopathology on day 9. (Scale bars: 200 μm in *Upper*; 50 μm in *Lower*.) (*E*) qRT-PCR analysis of relative mRNA expression levels of the indicated genes in whole colonic homogenates of untreated or DSS-treated mice on day 5. $*P < 0.05$; $**P < 0.01$.

responses, which was further verified by qRT-PCR analyses. As shown on a heat map, EZH2-deficient IECs isolated from DSS-treated mice produced significantly more proinflammatory cytokines and chemokines (Fig. 5*A*). Interestingly, Ingenuity Pathway Analysis (IPA) indicated that the genes altered in EZH2-deficient cells also were largely regulated by TNFα and IFNγ signaling, suggesting that EZH2 might exert its function through the regulation of these pathways (Fig. S3*A*).

To determine whether EZH2 regulates TNFα or IFNγ signaling in a cell-intrinsic manner, we isolated IECs from wild-type, EZH2$^{IEC-/-}$, and EZH2$^{IECOE/+}$ mice and treated them with TNFα or IFNγ. We found more prominent induction of TNFα-downstream genes in EZH2-deficient cells (Fig. 5*B*). Conversely, the overexpression of EZH2 diminished TNFα-induced gene expression (Fig. 5*B*). These results were experimentally reinforced by luciferase reporter assays and gene expression analyses using human colon cancer cell lines (Fig. S3 *B* and *C*). In contrast, EZH2 deficiency did not sensitize cells to IFNγ stimulation, as reflected by the finding of no clear difference in downstream gene expression and phosphorylated STAT1 levels between the conditions examined (Fig. S3 *D* and *E*). Taken together, our results suggest that EZH2 might modulate TNFα signaling to inhibit colitis, whereas the up-regulation of IFNγ signaling observed in EZH2-deficient cells is likely due to secondary effects.

We next sought to elucidate the molecular mechanism by which EZH2 modulates the induction of TNFα-regulated genes. To this end, we assessed the role of EZH2 in regulating TNFα-mediated activation of mitogen-activated protein kinases (MAPKs) and NF-κB (IκB) signaling. Using primary IECs from wild-type and EZH2$^{IEC-/-}$ mice after 3 d of DSS treatment, we found that EZH2 depletion enhanced the activating phosphorylation of IKKα/β, IκBα, p105, p65, ERK, and JNK (Fig. 5*C*). Conversely, the overexpression of EZH2 in IECs compromised TNFα-induced NF-κB activation in mice (Fig. S4*A*).

To further examine hyperactivated TNFα signaling in EZH2-deficient epithelia, we cultured primary IECs and stimulated them with TNFα, then assayed the levels of active/phosphorylated IKKα/β, NF-κB (phospho-p65 and phospho-p105, respectively), and JNK (Fig. 5*D*). We found no increase in NF-κB activation without TNFα treatment in cultured EZH2-deficient IECs, presumably owing to cell purities and the cultured cells' lack of TNFα secreted by immune cells. However, depletion of EZH2 rendered cells more sensitive to TNFα stimulation, as demonstrated by increased phosphorylation of IKKα/β, IκBα, JNK, p105, and p65 (Fig. 5*D*). In support of this finding, enhanced nuclear translocation of p50, p65, and c-Rel was detected in TNFα-stimulated EZH2-deficient cells (Fig. 5*E*). Accordingly, we found that compared with control cells, EZH2-overexpressing IECs exhibited attenuated pathway activation and gene induction on TNFα stimulation (Fig. S4*B*).

Given the important clinical relevance of these results, we assessed EZH2 and TNFα signaling activities with Gene Set Enrichment Analysis (GSEA) using patient sample data. We found that the repressive EZH2 signature (as defined by our gene expression profile) and the TNFα-activation signature were higher in inflamed IBD patients compared with noninflamed cohorts (using the GSE11223 dataset; Fig. 5*F*). More importantly, we found negative associations between EZH2 expression levels and TNFα activity in IBD patients (Fig. 5*G*). Of note, the cell cycle regulator cyclin-dependent kinase inhibitor 2A (CDKN2A) also has been identified as a direct target of PRC2 in multiple tissues, including the intestines. We also detected increased CDKN2A expression in EZH2-deficient IECs (Fig. S4*C*); however, epithelial cell proliferation was comparable in the wild-type and EZH2$^{IEC-/-}$ mice, suggesting that CDKN2A up-regulation is unlikely to be responsible for the colitis phenotype (Fig. S4*D*). Taken together, these results highlight that EZH2 acts upstream of NF-κB to antagonize TNFα signaling in experimental colitis.

EZH2 Modulates TRAF2/5 Expression to Compromise NF-κB Activation in Experimental Colitis. To further dissect the mechanism underlying how TNFα signaling becomes elevated in the absence of EZH2, we immunoprecipitated EZH2-bound chromatin from

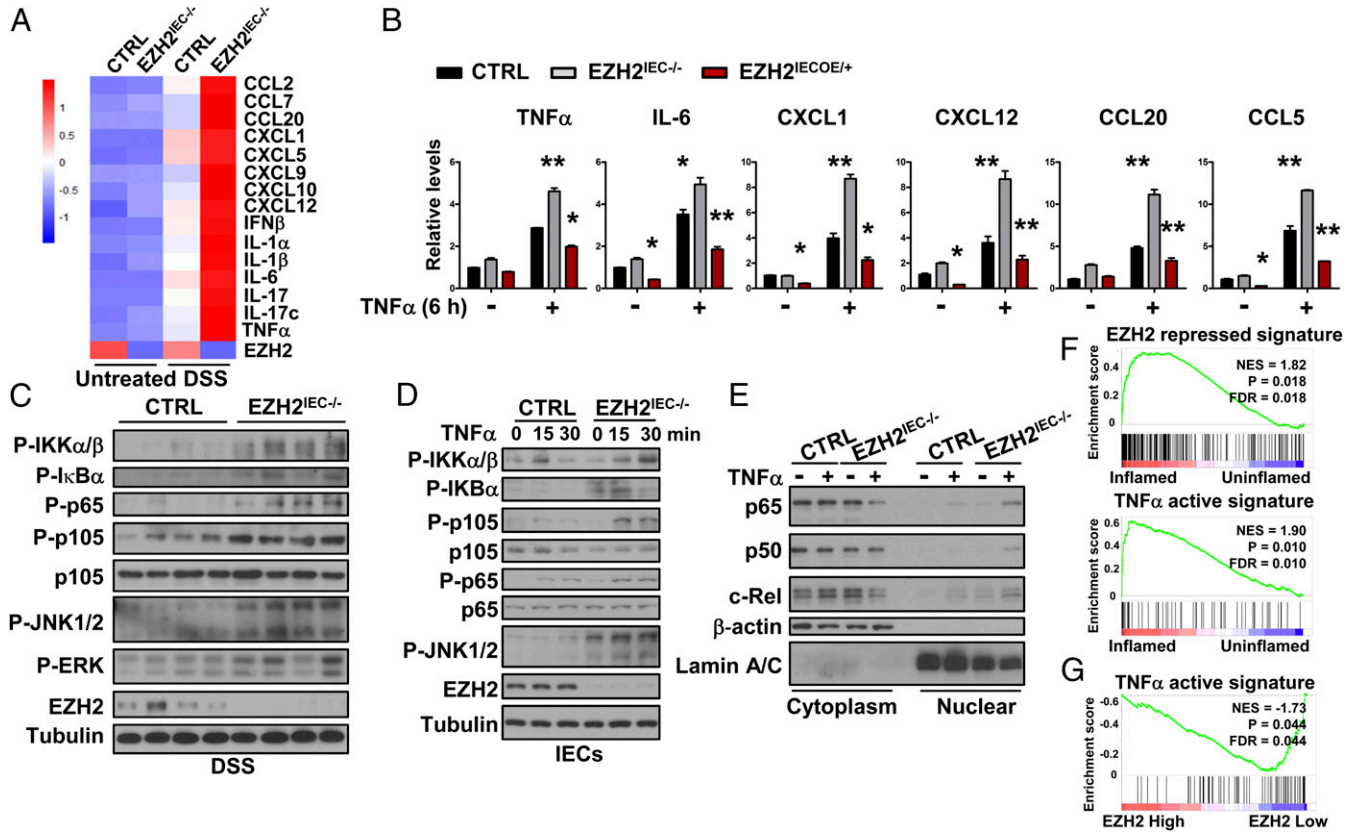

Fig. 5. Depletion of EZH2 stimulates TNFα signaling in experimental colitis. (*A*) qRT-PCR analysis of cytokines and chemokines in control (CTRL) and EZH2$^{IEC-/-}$ IECs with or without 3 d of DSS treatment. The results are summarized as a heat map. (*B*) Real-time PCR analysis of mRNA levels of TNFα target genes in IECs isolated from control, EZH2$^{IEC-/-}$, and EZH2$^{IECOE/+}$ mice after 6 h of TNFα treatment (50 ng/mL). *$P < 0.05$; **$P < 0.01$. (*C*) Western blot analysis of the indicated phosphoprotein or total protein in IECs isolated from control or EZH2$^{IEC-/-}$ mice treated for 5 d with DSS. (*D*) Western blot analysis of the indicated protein in primary IECs isolated from control and EZH2$^{IEC-/-}$ mice treated for 3 d with DSS after TNFα treatment for the indicated times. (*E*) Immunoblot analyses of the indicated proteins in cytoplasmic extracts and nuclear extracts from IECs stimulated with TNFα. (*F*) The EZH2 repressive signature (GSE84857) and TNFα active signature (GSE1474) were analyzed by GSEA in inflamed and noninflamed IBD patients (GSE11223; $n = 129$). (*G*) GSEA of EZH2 expression levels and TNFα active gene signature in IBD patients (GSE11223; $n = 66$). The IECs used in *A* and *C* were isolated using the EDTA method, whereas the IECs in *B*, *D*, and *E*, for treatment purposes, were obtained by enzymatic digestion.

wild-type IECs after 3 d of DSS treatment and analyzed the precipitated DNA with deep sequencing. There were 13,342 genes with EZH2 occupancy within 20 kb of the annotated genes. Of these regions, 82% were within the core transcribed portion of the genes, ±3 kb around the transcription start site (TSS) (Fig. S5 *A* and *B*). Annotation of the closest genes to the peaks showed that many peaks were positioned immediately after the TSS (Fig. 6*A*).

To correlate chromatin binding with direct gene regulation, we analyzed the EZH2-dependent transcriptome, with a primary focus on genes displaying up-regulation in the absence of EZH2. Among this group of 1,156 genes, 752 also contained EZH2 peaks (Fig. 6*B*). Interestingly, IPA identified several genes associated with the inflammatory response and gastrointestinal disease (Fig. S5*C*) that are notably implicated in TNFα signaling, including the TNF receptor-associated factor (TRAF) proteins TRAF2 and TRAF5. These EZH2 occupancies were shown in Genome Browser tracks and were readily validated by ChIP-qPCR assays (Fig. 6 *C* and *D*). As shown in Fig. 6*D*, EZH2 and the core PRC2 subunits SUZ12 and EED were recruited simultaneously to proximal promoter regions of *Traf2* and *Traf5* in IECs following DSS treatment. Furthermore, the expression levels of TRAF2 and TRAF5 exhibited twofold to fourfold increases in EZH2-depleted cells following 3 d of DSS treatment. In contrast, these proteins exhibited significantly reduced expression in EZH2$^{IECOE/+}$ mice compared with controls (Fig. 6*E*). Taken together, these results indicate that EZH2 directly inhibits the expression of key factors associated with TNFα signaling.

Intriguingly, the observed EZH2-mediated TRAF2/5 inhibition was inflammation-dependent, as evidenced by our finding that under steady-state conditions, TRAF5 expression was not altered by EZH2 knockout or overexpression. In fact, wild-type mice showed prominent stimulation of TRAF2/5 expression levels on DSS treatment (Fig. 6*E*). We performed ChIP-qPCR to examine whether and if so, how, histone modifications and promoter activity were altered at the *Traf2* and *Traf5* loci following inflammatory insults. Compared with the untreated state, H3K27me3, H3K4me3, and H3K9ac were increased at the core promoters of *Traf2* and *Traf5* on DSS treatment in wild-type cells (Fig. 6*F*). These patterns of seemingly opposing histone marks on the same promoter were defined as "bivalent" domains in a previous study (29). By exhibiting both active and repressive features (H3K4me3 and H3K27me3), bivalent genes are in a poised state, presumably allowing for their rapid activation on exposure to environmental stimuli. In accordance with this idea, we found that EZH2 fine-tunes TRAF2/5 expression in colitis; for example, EZH2 depletion caused a substantial reduction in H3K27me3 level, as predicted (Fig. 6*F*). More importantly, the H3K4me3 and H3K9ac histone marks were further elevated in DSS-treated EZH2-deficient cells compared with control cells (Fig. 6*F*). The poised state of the *Traf2* and *Traf5* loci in the mouse colitis model was reinforced by our gene expression

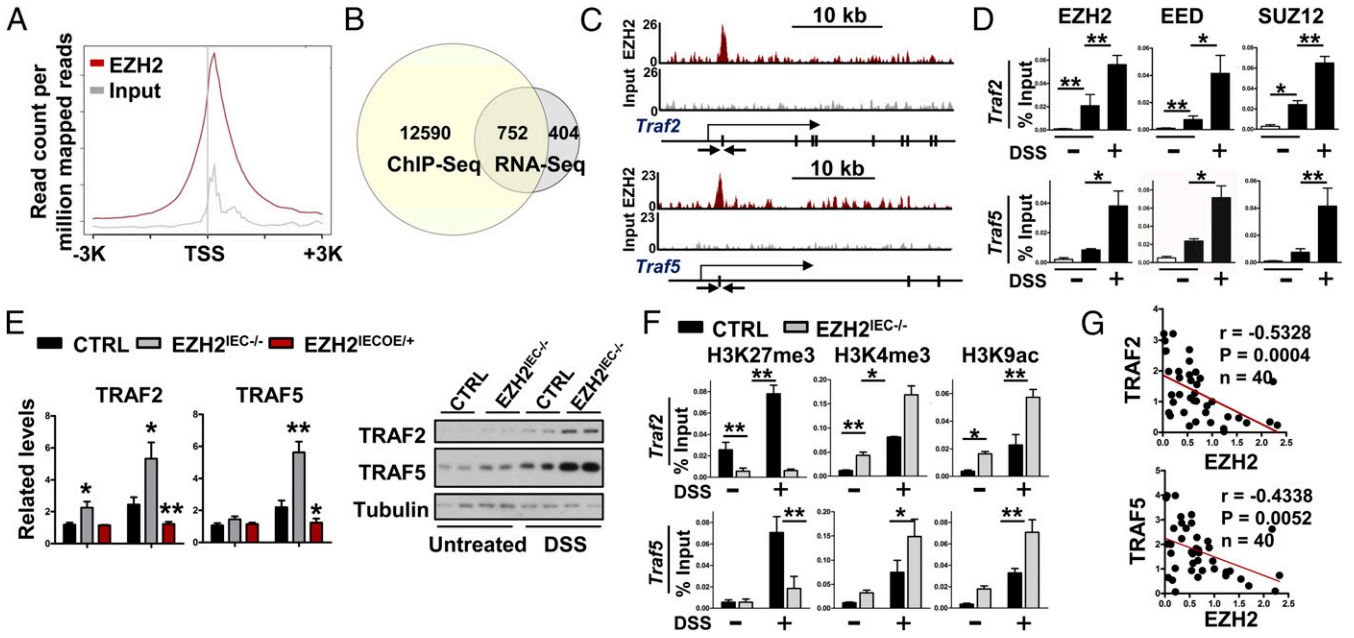

Fig. 6. EZH2 fine tunes TRAF2/5 expression to inhibit TNFα signaling in experimental colitis. (*A*) Average EZH2 ChIP signal across 13,342 annotated genes in IECs isolated from wild-type mice treated for 3 d with DSS. (*B*) Venn diagram showing the numbers of genes harboring EZH2 peaks and displaying up-regulation in EZH2-KO IECs. (*C*) Snapshot of the EZH2 ChIP-Seq signal at the *Traf2* and *Traf5* loci in IECs isolated from DSS-treated (3 d) wild-type mice. The arrow indicates the location of the ChIP primer pairs. (*D*) ChIP-qPCR analysis of EZH2, EED, and SUZ12 binding to *Traf2* and *Traf5* loci in IECs isolated from wild-type mice with or without DSS treatment. (*E*) qRT-PCR analysis (*Left*) and Western blot analysis (*Right*) of TRAF2 and TRAF5 expression in IECs as indicated. (*F*) ChIP-qPCR analysis of H3K27me3, H3K4me3, and H3K9ac modifications at the *Traf2* and *Traf5* promoters in IECs. (*G*) Correlation between EZH2 and TRAF2/5 expression level in IBD specimens. Statistical significance was determined using the Pearson correlation coefficient. $*P < 0.05$; $**P < 0.01$. The IECs used in this figure were isolated using EDTA.

analysis showing that depletion of EZH2 following DSS treatment further enhanced TRAF2 and TRAF5 expression (Fig. 6*F*). The functional importance of this regulation of TRAF2/5 by EZH2 was supported by clinical specimen analysis. Specifically, qRT-PCR analysis of colitis patient specimens indicated significant and negative associations between the mRNA levels of EZH2 and TRAF2 or TRAF5 (Fig. 6*G*). Taken together, these results demonstrate that EZH2 fine tunes TRAF2/5 expression to modulate NF-κB activation in experimental colitis.

EZH2 Inhibits TNFα-Mediated Cell Death. Given that epithelial apoptosis is one of the major causes of colitis, and that the epithelial barrier is disrupted in the absence of EZH2 (Fig. 2 *E* and *F*), we assessed for defects in epithelial cell survival in $EZH2^{IEC-/-}$ mice. Eliminating the possibility that the loss of EZH2 enhances NF-κB signaling, which would presumably sustain cell survival, both TUNEL- and cleaved caspase 3-positive staining was significantly higher in the colon sections of $EZH2^{IEC-/-}$ mice (Fig. 7*A*). This observation was strengthened by Western blot assays showing markedly enhanced signaling intensities of cleaved caspase 3 and cleaved PARP in $EZH2^{IEC-/-}$ mice compared with control mice (Fig. 7*B*).

We next established intestinal organoid cultures to assess whether the loss of EZH2 induces apoptosis in a cell-intrinsic manner. 7-aminoactinomycin D (7-AAD) whole-mount staining revealed slightly more apoptosis in EZH2-depleted cells than in control cells (Fig. 7*C*). Interestingly, we noticed that TNFα administration induced massive apoptosis and reductions in the size of EZH2-depleted organoids, with a much smaller effect on the control organoid cultures (Fig. 7*C*). Furthermore, immunoblotting analyses revealed significantly higher cleaved caspase 8 and caspase 3 signals in EZH2-silenced IECs (Fig. 7*D*). These results emphasize that the loss of EZH2 enhances cellular sensitivity to TNFα-induced apoptosis.

EZH2 Down-Regulation Promotes Apoptosis by Regulating ITCH-Mediated Degradation of c-FLIP. Given that NF-κB signaling is primarily prosurvival, it is puzzling that EZH2-deficent IECs are more prone to apoptosis while exhibiting enhanced NF-κB signaling. NF-κB activation sustains cell survival predominately through the induction of c-FLIP expression, thereby diminishing TNFα-induced caspase 8 cleavage (12). To better understand this seemingly contradictory observation, we examined c-FLIP expression in the absence of EZH2. In support of the possibility that NF-κB activates c-FLIP transcription, we observed a slightly higher relative abundance of c-FLIP mRNA in $EZH2^{IEC-/-}$ mice compared with wild-type mice (Fig. 8*A*, *Left*). Surprisingly, the protein levels of c-FLIP exhibited the opposite trend, with the IECs of $EZH2^{IEC-/-}$ mice showing significantly less protein expression. Conversely, EZH2-overexpressing mice produced markedly more c-FLIP protein (Fig. 8*A*, *Right*). These results suggest a posttranscriptional mechanism by which EZH2 regulates c-FLIP expression in colitis. In agreement with this hypothesis, TNFα-mediated c-FLIP protein stability, rather than transcriptional activation, was compromised in EZH2-deficient IECs (Fig. 8*B* and Fig. S6*A*). Moreover, MG132 treatment of EZH2-deficient cells restored c-FLIP protein to a level similar as that in control cells (Fig. 8*B*), confirming that EZH2 regulates the stability of c-FLIP via the 26S proteasome.

Focusing on the candidate E3 ligases that govern c-FLIP stability, we found that both mRNA and protein levels of itchy E3 ubiquitin protein ligase (ITCH) were significantly increased in the absence of EZH2 (Fig. 8*A* and Fig. S6 *B* and *C*), whereas ectopically expressed EZH2 inhibited ITCH production in IECs (Fig. 8*A*, *Right*). More importantly, ChIP-Seq analysis suggested that *Itch* was directly regulated by EZH2, as revealed by Genome Browser tracks (Fig. 8*C*). Thus, we conducted a ChIP-qPCR assay to examine the occupancy of EZH2 at the *Itch* locus. The results indicated that EZH2 and other PRC2 complex

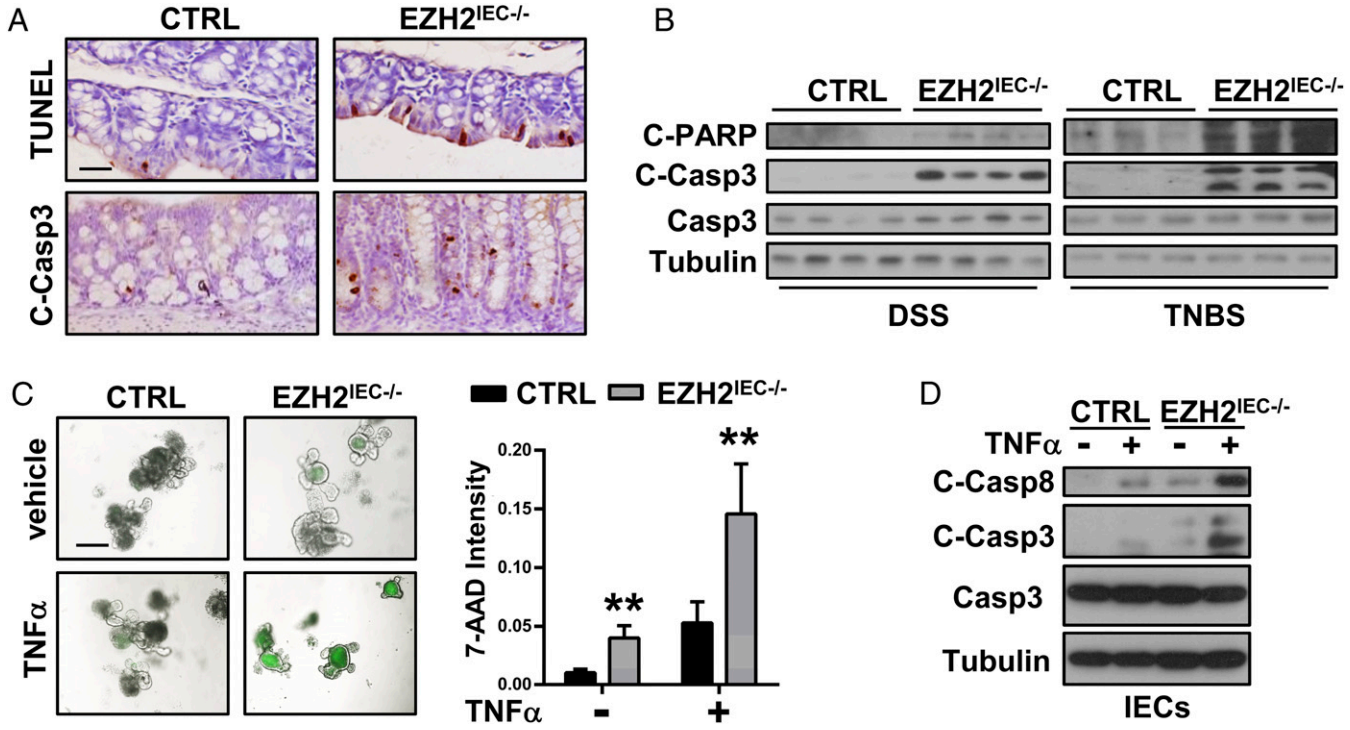

Fig. 7. Loss of EZH2 enhances TNFα-induced apoptosis. (*A*) TUNEL and cleaved caspase 3 staining of colon sections from DSS-treated (5 d) control (CTRL) and EZH2$^{IEC-/-}$ mice. (*B*) Western blot analysis of the indicated protein in IECs isolated from of DSS- or TNBS-treated (5 d) control and EZH2$^{IEC-/-}$ mice (EDTA isolation). (*C*) Intestinal organoids derived from wild-type and EZH2$^{IEC-/-}$ mice. (*Left*) After 5 d of differentiation, the organoids were treated with or without recombinant mouse TNFα for 16 h, and 7-AAD-stained organoids (green) were imaged. (*Right*) Quantitation of the fluorescence density per organoid. (*D*) Immunoblot analysis of cleaved and total caspases in IECs (isolated by enzyme digestion) after TNFα administration, as indicated.

members (SUZ12 and EED) were simultaneously recruited to the promoter region of *Itch* in wild-type IECs (Fig. 8*D*). We also found that EZH2 ablation reduced H3K27me3 and increased H3K4me3 and H3K9ac within the *Itch* promoter (Fig. 8*E*), suggesting the occurrence of chromatin conformational remodeling to a more active state at this locus in the absence of EZH2.

Given that long-term culture of IECs is not feasible, we performed rescue experiments using mouse embryonic fibroblasts (MEFs) to assess whether the increased ITCH expression in EZH2-depleted cells indeed caused the reduction of c-FLIP expression and cell death. We found that depletion of the increased ITCH expression by siRNA restored TNFα-induced c-FLIP expression in EZH2-deficient cells (Fig. 8*F*). Moreover, apoptosis was decreased in this condition, as determined by reductions in cleaved-caspase 3 and annexin V levels (Fig. 8 *F* and *G*). Taken together, our results indicate that EZH2 ablation sensitizes IECs to TNFα-mediated NF-κB activation while maintaining low levels of c-FLIP, thereby making cells prone to apoptosis.

Discussion

TNFα is known to be involved in IBD through regulation of the chronic inflammatory response and the apoptosis of IECs. However, despite its name, which references necrotic cell death, TNFα does not efficiently induce apoptosis under physiological conditions. This effect can be explained by TNFα's simultaneous induction of NF-κB, which induces a set of prosurvival proteins, including c-FLIP, to constrain caspase 8 activation. Therefore, how the multifaceted functions of TNFα are coordinated to drive IBD pathogenesis remains to be defined. Here, we show that EZH2 integrates the complex functions of TNFα to enhance the inflammatory response and apoptosis in the context of colitis (Fig. 8*H*), suggesting that IBD patients with lower levels of EZH2 might have better clinical responses to anti-TNFα treatment. As stated above, EZH2 represents an attractive target for chemical inhibition due to its role in cancer. Inflammation is closely associated with tumorigenesis, and IBD is a predisposing factor for colorectal cancer. The present study indicated that EZH2 suppresses inflammation-associated epithelial damage while positively promoting oncogenic transformation, as reported previously (30–32). Thus, the roles of EZH2 in inflammation-induced colorectal cancer merit further study.

Inflammatory bowel disease and experimentally induced intestinal inflammation are characterized by NF-κB activation and increased expression of proinflammatory NF-κB target genes. However, NF-κB has not only proinflammatory functions, but also tissue-protective functions, especially within intestinal epithelium. Thus, genetic ablation of the regulatory subunits IKKγ (the central kinase complex required for NF-κB activation), IKKα, and IKKβ in IECs causes spontaneous murine colitis (33, 34). NF-κB exerts its prosurvival function through up-regulation of a subset of proteins, including Bcl-xl, c-IAP1/2, x-IAP, and c-FLIP, of which c-FLIP is the best known (12, 35–37). c-FLIP is a catalytically inactive caspase 8/10 homolog capable of inhibiting caspase 8 recruitment to block apoptotic processes. In the context of IBD, how IECs circumvent the antiapoptotic actions of NF-κB to enable TNFα-induced cell death is unknown. Our study indicates that EZH2 loss may explain these seemingly contradictory results. In the absence of EZH2, the prosurvival activity of NF-κB is dissociated from its proinflammatory activity, and cells are simultaneously sensitized to caspase 8-mediated apoptosis (Fig. 8*H*).

The core members of the PRC2 complex include the methyltransferase EZH2, EED, SUZ12, and RBBP7/4. The enzymatic activity of this complex mediates the trimethylation of lysine 27 on histone H3 (H3K27me3) and leads to transcriptional

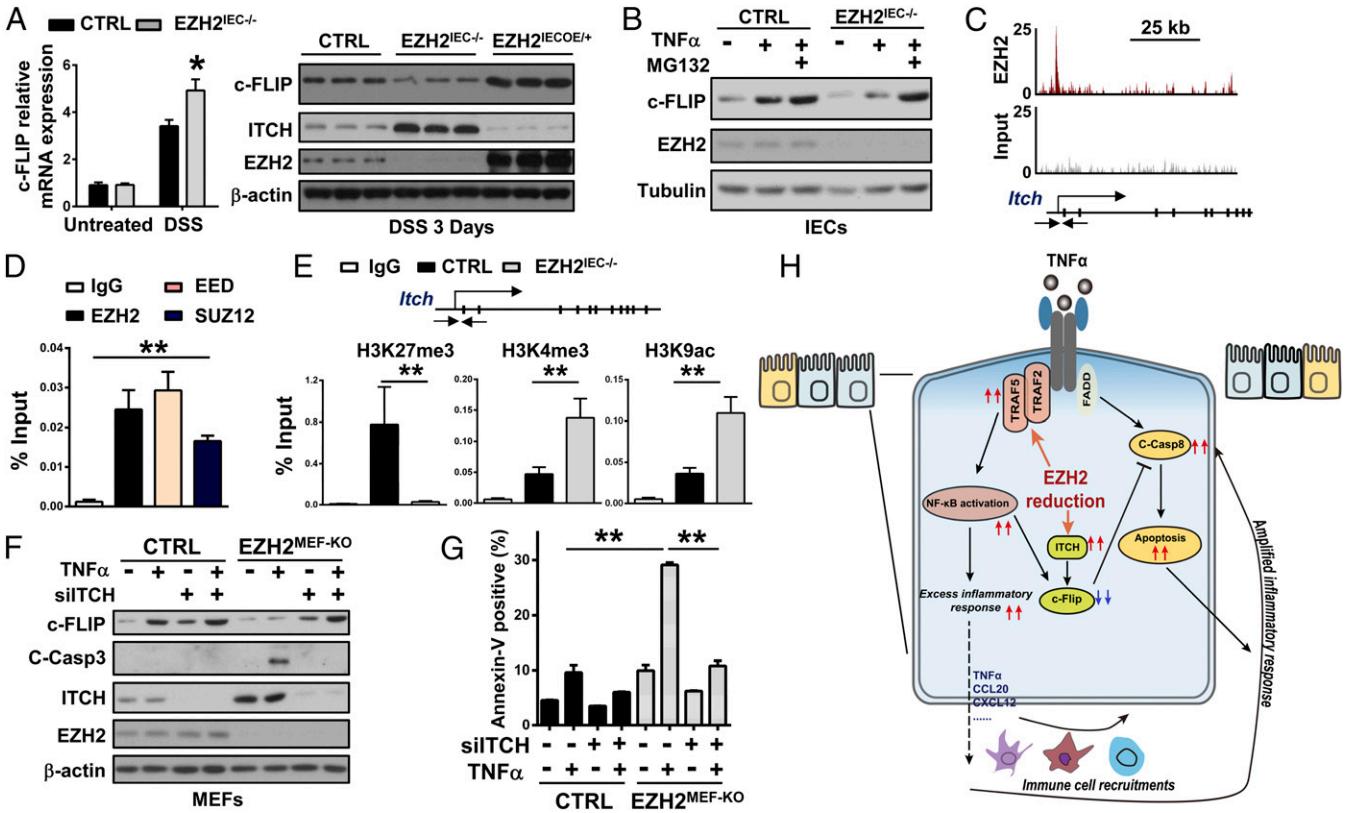

Fig. 8. Loss of EZH2 enhances apoptosis through the up-regulation of ITCH to induce c-FLIP degradation. (*A*) qRT-PCR analysis of c-FLIP mRNA in IECs isolated from untreated or DSS-treated (3 d) mice (*Left*), and immunoblot analysis of the indicated protein in the IECs of DSS-treated (3 d) wild-type (CTRL), EZH2$^{IEC-/-}$, and EZH2$^{IECOE/+}$ mice (*Right*). (*B*) Immunoblot analysis of the indicated protein in IECs isolated from wild-type and EZH2$^{IEC-/-}$ mice treated with TNFα (24 h) with or without MG132 administration. (*C*) Snapshot of EZH2 ChIP-Seq signal at the *Itch* loci in IECs isolated from DSS-treated mice. The arrow indicates the location of ChIP-qPCR primer pairs. (*D*) ChIP-qPCR analysis of EZH2, EED, and SUZ12 binding to the *Itch* locus. (*E*) ChIP-qPCR analysis of H3K27me3, H3K4me3, and H3K9ac markers for the *Itch* locus in IECs isolated from wild-type and EZH2$^{IEC-/-}$ mice. (*F* and *G*) Western blot analysis of the indicated proteins (*F*) and quantitative results of annexin-V staining (*G*) in MEFs with or without ITCH siRNA transfection. (*H*) Model depicting how EZH2 loss promotes disruption of intestinal barrier homeostasis in colitis. The IECs used in *A*, *C*, *D*, and *E* were isolated using the EDTA method, whereas the IECs used in *B* were isolated by enzymatic digestion. $*P < 0.05$; $**P < 0.01$.

repression of target genes (38, 39). In a recently reported study, EED was found to regulate intestinal homeostasis, and EED KO mice showed defects in stem cell proliferation and lineage differentiation in the steady state (22, 24). This phenotype makes this mouse model impractical for studying the role of PRC2 in colitis. Interestingly, the PRC2 catalytic subunit EZH2 is dispensable for steady-state intestinal homeostasis but is required for the suppression of colitis pathogenesis. Genome-wide mapping studies of chromatin modifications have revealed that the promoters of many of the genes critical for development and pathological transformation harbor a distinctive histone modification signature termed bivalency, which combines the activating H3K4me3 and the repressive H3K27me3 markers (40, 41). Previous work has revealed that PRC2 specifically represses genes with bivalent promoters in the adult intestine (23). Our data support and expand this idea, revealing that the promoters of both *Traf2* and *Traf5* are bivalent during colitis, with both H3K4me3 and H3K27me3 increased on DSS treatment. During disease progression, EZH2 reduction leads to a loss of repressive markers, leading to induction of TRAF2/5 expression and augmenting TNFα-mediated NF-κB signaling. Notably, the upstream signal that governs the down-regulation of EZH2 in IBD remains to be identified. This information will facilitate an understanding of how the intestinal microbiota, immune system, genetic factors, and specific environmental factors contribute to IBD.

In conclusion, our results indicate that EZH2 functions as a primary defense mechanism to maintain an intact and functional mucosal barrier by modulating TNFα-mediated intestinal inflammation and apoptosis. These results are potentially relevant with respect to disease intervention.

Experimental Procedures

Detailed information on expression plasmids, shRNAs, cell culture, immunohistochemistry, histology, qRT-PCR, ChIP-qPCR, GSEA, and primers is provided in *SI Experimental Procedures*.

Mice. All mice were maintained in a specific-pathogen-free facility, and all procedures were performed in compliance with *Guide for the Care and Use of Laboratory Animals* (42). Moreover, all procedures were approved by the institutional Biomedical Research Ethics Committee, Shanghai Institutes for Biological Sciences, Chinese Academy of Sciences. EZH2$^{IEC-/-}$mice were generated by crossing EZH2 Flox mice (43) with Villin-Cre mice (44). EZH2-overexpressing mice (EZH2$^{OE/+}$) were generated by our group as described previously (45). All mice were backcrossed with C57BL/6 mice for at least seven generations, and littermates were used as controls in all experiments.

Human Specimen Analysis. Patients with IBD and non-IBD control subjects for this study were recruited from Fudan University Shanghai Cancer Center. The diagnosis of CD or UC was based on a standard combination of clinical, endoscopic, histological, and radiologic criteria. The use of pathological specimens, as well as the review of all pertinent patient records, were approved by the Ethics Review Board of Fudan University Shanghai Cancer Center. Immunohistochemical analyses were performed as described previously (45) using a specific anti-EZH2 antibody (Cell Signaling Technology). Protein expression was scored and quantified by pathologists who were blinded to the outcome of the cases. In brief, the quantification was based

on a multiplicative index of the average staining intensity (0–3) and the extent of staining (0–3) in the cores. This scoring system yielded a 10-point staining index that ranged from 0 (no staining) to 9 (extensive; strong staining). Tissue RNA from colonic mucosal biopsy specimens from patients with IBD was also prepared for the analysis of transcript levels.

DSS- and TNBS-Induced Colitis. To induce colitis, littermate mice (6-8 wk older) were fed 3% DSS (MP Biomedicals) for 6 d, followed by 3 d of regular drinking water. For permeability experiments, FITC-conjugated dextran (4,000 MW) was gavaged at 2 mg/10 g of body weight. For the TNBS model, overnight-fasted mice were treated with 150 mg/kg TNBS (Sigma-Aldrich) via intrarectal injection.

IECs Isolation. For RNA-Seq and ChIP-Seq analyses, IECs from mice treated with DSS for 3 d were isolated using isolation buffer (30 mM EDTA and 1 mM DTT). For ligand stimulation experiments, the colons were incubated with collagenase type I (250 ng/mL; Sigma-Aldrich) and Dispase II (440 ng/mL; Sigma-Aldrich) for 2 h. After repeated washes, the cells were plated in dishes coated with type I collagen overnight. The next day, the cells were treated with TNFα (50 ng/mL; PeproTech) or IFNγ (20 ng/mL; PeproTech). Epithelial cell purities from the EDTA-based and enzymatic digests were ∼95% and 80%, respectively, using an EpCAM antibody and FACS analysis.

RNA-Seq Analysis. Each group of IECs was isolated from three to five animals using EDTA-based isolation. RNA from wild-type and EZH2-deficient IECs was subjected to HiSeq RNA-Seq, performed by BGI Tech Solutions. Transcriptomic reads from the RNA-Seq experiments were mapped to a reference genome (mm10) using Bowtie. Gene expression levels were quantified using the RSEM software package. The list of significantly affected genes was obtained by setting a false discovery rate (FDR) threshold of 0.001 and fold changes ≥1.5. The raw data can be downloaded as GSE84857. Differentially expressed genes were subsequently analyzed using the DAVID bioinformatics platform and IPA.

ChIP-Seq Assay. Wild-type IECs were isolated from five mice after 3 d of DSS treatment. The chromatin was prepared and ChIP-Seq analysis was performed by Active Motif, using an antibody against EZH2 (Active Motif). Seventy-five nucleotide reads generated by Illumina sequencing were mapped to the genome using the BWA algorithm with default settings. Only reads that passed the Illumina purity filter, that aligned with no more than two mismatches, and that mapped uniquely to the genome were used in the subsequent analysis. Of the total reads, 12756 peaks were identified over the input control. The heat maps and average profile for RefSeq gene bodies were generated using ngsplot v2.61. The raw data can be downloaded as GSE84858.

Statistical Analysis. All experiments were performed using 3–15 mice or three independent repeated experiments, including Western blot, qRT-PCR, and ChIP-qPCR analyses. Unless indicated otherwise, data are presented as mean ± SEM, and statistical significance was determined using a two-tailed Student *t* test. The Pearson correlation coefficient was used to evaluate the relationship between EZH2 and gene expression, and the Wilcoxon signed-rank test was used for patient analysis. In the figures, $*P < 0.05$; $**P < 0.01$. The RNA-Seq and ChIP-Seq data have been deposited in the Gene Expression Omnibus database under accession numbers GSE84857 and GSE84858.

ACKNOWLEDGMENTS. This work was supported by grants from the National Natural Science Foundation of China (31471281 and 81422030, to J.Q.; 81502440, to M.J.; and 31570881, to X.W.), the Strategic Priority Research Program of the Chinese Academy of Sciences (XDB19000000), the National Key Basic Research Program (2016YFC0902202), the Thousand Talents Plan (Youth; J.Q.), the Open Fund of the State Key Laboratory of Pharmaceutical Biotechnology, Nanjing University (KF-GN-201602), and the State Key Laboratory of Medical Genomics, Collaborative Innovation Center of Systems Biomedicine, Shanghai Jiao Tong University School of Medicine.

1. Maloy KJ, Powrie F (2011) Intestinal homeostasis and its breakdown in inflammatory bowel disease. *Nature* 474:298–306.
2. Alenghat T, et al. (2013) Histone deacetylase 3 coordinates commensal-bacteria-dependent intestinal homeostasis. *Nature* 504:153–157.
3. Vereecke L, et al. (2014) A20 controls intestinal homeostasis through cell-specific activities. *Nat Commun* 5:5103.
4. Günther C, Neumann H, Neurath MF, Becker C (2013) Apoptosis, necrosis and necroptosis: Cell death regulation in the intestinal epithelium. *Gut* 62:1062–1071.
5. Hand TW (2015) Interleukin-18: The bouncer at the mucosal bar. *Cell* 163:1310–1312.
6. Nowarski R, et al. (2015) Epithelial IL-18 equilibrium controls barrier function in colitis. *Cell* 163:1444–1456.
7. Xu J, et al. (2016) The REGγ-proteasome forms a regulatory circuit with IκBε and NFκB in experimental colitis. *Nat Commun* 7:10761.
8. Visekruna A, et al. (2006) Proteasome-mediated degradation of IkappaBalpha and processing of p105 in Crohn disease and ulcerative colitis. *J Clin Invest* 116:3195–3203.
9. Lin W, et al. (2017) Raf kinase inhibitor protein mediates intestinal epithelial cell apoptosis and promotes IBDs in humans and mice. *Gut* 66:597–610.
10. Gerich ME, McGovern DP (2014) Towards personalized care in IBD. *Nat Rev Gastroenterol Hepatol* 11:287–299.
11. Qiu W, et al. (2011) PUMA-mediated intestinal epithelial apoptosis contributes to ulcerative colitis in humans and mice. *J Clin Invest* 121:1722–1732.
12. Chang L, et al. (2006) The E3 ubiquitin ligase itch couples JNK activation to TNFalpha-induced cell death by inducing c-FLIP(L) turnover. *Cell* 124:601–613.
13. Däbritz J, Menheniott TR (2014) Linking immunity, epigenetics, and cancer in inflammatory bowel disease. *Inflamm Bowel Dis* 20:1638–1654.
14. Theodoris CV, et al. (2015) Human disease modeling reveals integrated transcriptional and epigenetic mechanisms of NOTCH1 haploinsufficiency. *Cell* 160:1072–1086.
15. Häsler R, et al. (2012) A functional methylome map of ulcerative colitis. *Genome Res* 22:2130–2137.
16. Cooke J, et al. (2012) Mucosal genome-wide methylation changes in inflammatory bowel disease. *Inflamm Bowel Dis* 18:2128–2137.
17. Allan RS, et al. (2012) An epigenetic silencing pathway controlling T helper 2 cell lineage commitment. *Nature* 487:249–253.
18. Levy D, et al. (2011) Lysine methylation of the NF-κB subunit RelA by SETD6 couples activity of the histone methyltransferase GLP at chromatin to tonic repression of NF-κB signaling. *Nat Immunol* 12:29–36.
19. Stender JD, et al. (2012) Control of proinflammatory gene programs by regulated trimethylation and demethylation of histone H4K20. *Mol Cell* 48:28–38.
20. Takeshima H, et al. (2012) Induction of aberrant trimethylation of histone H3 lysine 27 by inflammation in mouse colonic epithelial cells. *Carcinogenesis* 33:2384–2390.
21. Margueron R, Reinberg D (2011) The Polycomb complex PRC2 and its mark in life. *Nature* 469:343–349.
22. Chiacchiera F, Rossi A, Jammula S, Zanotti M, Pasini D (2016) PRC2 preserves intestinal progenitors and restricts secretory lineage commitment. *EMBO J* 35:2301–2314.
23. Jadhav U, et al. (2016) Acquired tissue-specific promoter bivalency is a basis for PRC2 necessity in adult cells. *Cell* 165:1389–1400.
24. Koppens MAJ, et al. (2016) Deletion of Polycomb Repressive Complex 2 from mouse intestine causes loss of stem cells. *Gastroenterology* 151:684–697.e12.
25. Zhu H, et al. (2015) Computational prediction and validation of BAHD1 as a novel molecule for ulcerative colitis. *Sci Rep* 5:12227.
26. Kitajima S, Takuma S, Morimoto M (1999) Changes in colonic mucosal permeability in mouse colitis induced with dextran sulfate sodium. *Exp Anim* 48:137–143.
27. Fiorucci S, et al. (2002) Importance of innate immunity and collagen binding integrin alpha1beta1 in TNBS-induced colitis. *Immunity* 17:769–780.
28. Liu W, et al. (2013) Intestinal epithelial vitamin D receptor signaling inhibits experimental colitis. *J Clin Invest* 123:3983–3996.
29. Voigt P, Tee WW, Reinberg D (2013) A double take on bivalent promoters. *Genes Dev* 27:1318–1338.
30. Kim E, et al. (2013) Phosphorylation of EZH2 activates STAT3 signaling via STAT3 methylation and promotes tumorigenicity of glioblastoma stem-like cells. *Cancer Cell* 23:839–852.
31. Cha TL, et al. (2005) Akt-mediated phosphorylation of EZH2 suppresses methylation of lysine 27 in histone H3. *Science* 310:306–310.
32. Bracken AP, et al. (2003) EZH2 is downstream of the pRB-E2F pathway, essential for proliferation and amplified in cancer. *EMBO J* 22:5323–5335.
33. Greten FR, et al. (2004) IKKbeta links inflammation and tumorigenesis in a mouse model of colitis-associated cancer. *Cell* 118:285–296.
34. Nenci A, et al. (2007) Epithelial NEMO links innate immunity to chronic intestinal inflammation. *Nature* 446:557–561.
35. Wang CY, Mayo MW, Korneluk RG, Goeddel DV, Baldwin AS, Jr (1998) NF-kappaB antiapoptosis: Induction of TRAF1 and TRAF2 and c-IAP1 and c-IAP2 to suppress caspase 8 activation. *Science* 281:1680–1683.
36. Ravi R, et al. (2001) Regulation of death receptor expression and TRAIL/Apo2L-induced apoptosis by NF-kappaB. *Nat Cell Biol* 3:409–416.
37. Tang G, et al. (2001) Inhibition of JNK activation through NF-kappaB target genes. *Nature* 414:313–317.
38. Margueron R, et al. (2008) Ezh1 and Ezh2 maintain repressive chromatin through different mechanisms. *Mol Cell* 32:503–518.
39. Delgado-Olguín P, et al. (2012) Epigenetic repression of cardiac progenitor gene expression by Ezh2 is required for postnatal cardiac homeostasis. *Nat Genet* 44:343–347.
40. Weiner A, et al. (2016) Co-ChIP enables genome-wide mapping of histone mark co-occurrence at single-molecule resolution. *Nat Biotechnol* 34:953–961.
41. Béguelin W, et al. (2016) EZH2 and BCL6 cooperate to assemble CBX8-BCOR complex to repress bivalent promoters, mediate germinal center formation and lymphomagenesis. *Cancer Cell* 30:197–213.
42. National Research Council (2011) *Guide for the Care and Use of Laboratory Animals* (National Academies Press, Washington, DC), 8th Ed.
43. Su IH, et al. (2003) Ezh2 controls B cell development through histone H3 methylation and Igh rearrangement. *Nat Immunol* 4:124–131.
44. Madison BB, et al. (2002) Cis elements of the villin gene control expression in restricted domains of the vertical (crypt) and horizontal (duodenum, cecum) axes of the intestine. *J Biol Chem* 277:33275–33283.
45. Qin J, et al. (2013) COUP-TFII inhibits TGF-β-induced growth barrier to promote prostate tumorigenesis. *Nature* 493:236–240.